Dynamics of a Bose-Einstein condensate near a Feshbach resonance

R. A. Duine* and H. T. C. Stoof†
Institute for Theoretical Physics, University of Utrecht, Leuvenlaan 4, 3584 CE Utrecht, The Netherlands
(Received 22 November 2002; published 9 July 2003)

We discuss the response of a Bose-Einstein condensate to a change in the scattering length, which is experimentally realized by tuning the magnetic field near a Feshbach resonance. In particular, we consider the collapse of the condensate induced by a sudden change in the scattering length from a large positive to a small negative value. We also consider the condensate dynamics that results from a single pulse in the magnetic field, due to which the scattering length is rapidly increased from zero to a large value and then after some time rapidly decreased again to its initial value. We focus primarily on the consequences of the quantum evaporation process on the dynamics of the Bose-Einstein condensate, but also discuss the effects of atom-molecule coherence.

DOI: 10.1103/PhysRevA.68.013602 PACS number(s): 03.75.Kk, 67.40.−w, 32.80.Pj

I. INTRODUCTION

From single-channel scattering theory, it is well known that the collisional cross section changes dramatically if the energy of the incoming particles is close to the energy of a long-lived bound state in the interaction potential. In particular, the magnitude of the *s*-wave scattering length a of an attractive potential well diverges as the depth of the potential well is increased such that a new bound state enters the well [1]. A similar behavior occurs in the case of a Feshbach resonance, when the energy of the two particles in the incoming channel is close to the energy of a bound state in a closed channel [2]. In the case of collisions between alkali atoms, the coupling between the two channels is provided by the hyperfine interaction. Due to the spin flips involved in this interaction, the difference in energy between the bound state and the continuum, the so-called detuning, is adjustable by means of a magnetic bias field. Feshbach resonances were first predicted theoretically [3,4], but have now also been observed experimentally, in various atomic species [5–8]. As a result, the experiments with magnetically trapped ultracold atomic gases, where the *s*-wave scattering length fully determines the interaction effects, have an unprecedented high level of control over the interatomic interactions. In this paper, we focus on ^{85}Rb in the $f=2, m_f=-2$ hyperfine state, which has a Feshbach resonance at a magnetic field of $B_0 \approx 154.9$ G [9]. Near the resonance the scattering length, as a function of magnetic field, is given by

$$a(B) = a_{\rm bg}\left(1 - \frac{\Delta B}{B - B_0}\right). \tag{1}$$

The resonance is characterized by the width $\Delta B \approx 11.6$ G and the off-resonant background scattering length $a_{\rm bg} \approx -450 a_0$, with a_0 the Bohr radius. In Fig. 1, the scattering length is shown as a function of the magnetic field. Clearly, it can be adjusted experimentally from large negative values, to large positive ones. Moreover, at a magnetic field of $B \approx 166.5$ G the scattering length vanishes, and the gas behaves effectively as an ideal Bose gas.

With this experimental degree of freedom, it is possible to study very interesting new regimes in the many-body physics of ultracold atomic gases. The first experimental application was the detailed study of the collapse of a condensate with attractive interactions. In general, a collapse occurs when the attractive interactions overcome the kinetic energy of the condensate atoms in the trap. Since the typical interaction energy is proportional to the density, there is a certain maximum number of atoms above which the condensate is unstable [10–14]. In the first observations of the condensate collapse by Bradley *et al.* [15], a condensate of doubly spin-polarized ^{7}Li atoms was used. These atoms have a magnetic-field independent scattering length of $a \approx -27 a_0$. For the experimental trap parameters, this leads to a maximum number of condensate atoms that was so low that nondestructive imaging of the condensate was impossible. Moreover, thermal fluctuations due to a large thermal component make the

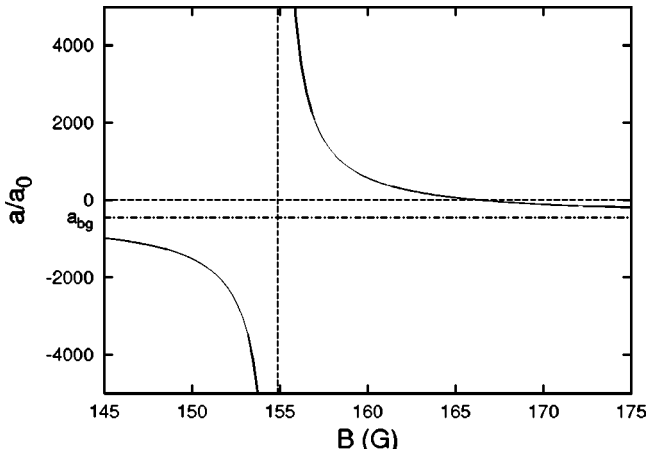

FIG. 1. The scattering length as a function of the magnetic field for ^{85}Rb in the state $|f=2; m_f=-2\rangle$. The position of the resonance is indicated by the vertical dashed line. At the horizontal dashed line, the scattering length vanishes. The dash-dotted line indicates the background scattering length $a_{\rm bg} \approx -450 a_0$.

*Electronic address: duine@phys.uu.nl;
URL: http://www.phys.uu.nl/~duine/bec
†Email address: stoof@phys.uu.nl;
URL: http://www.phys.uu.nl/~stoof

initiation of the collapse a stochastic process, thus preventing also a series of destructive measurements of a single-collapse event [16–18]. A statistical analysis, has nevertheless, resulted in important information about the collapse process. Very recently, it was even possible to overcome these problems [19].

In addition to the experiment with ^{7}Li, experiments with ^{85}Rb have been carried out. In particular, Roberts *et al.* [20] also studied the stability criterion for the condensate, and Donley *et al.* [21] studied the dynamics of a single-collapse event in great detail. Both of these experiments make use of the above-mentioned Feshbach resonance to achieve a well-defined initial condition for each destructive measurement. It turns out that during a collapse, a significant fraction of atoms is expelled from the condensate. Moreover, one observes a burst of hot atoms with an energy of about 150 nK. Several mean-field analyses of the collapse, which model the atom loss phenomenologically by a three-body recombination rate constant, have offered some theoretical insight [22–27]. However, the physical mechanism responsible for the explosion of atoms out of the condensate and the formation of the noncondensed component is still largely ununderstood at present.

A second experimental application of the Feshbach resonance has been implemented by Claussen *et al.* [33]. Starting from the noninteracting limit, the scattering length is made to jump very fast back and forth to a large and positive value. Surprisingly, in this case one also observes loss of atoms from the condensate, as well as a burst of hot atoms. Even more surprising is the fact that the amount of atoms expelled from the Bose-Einstein condensate decreases with time during some intervals, excluding a theoretical explanation in terms of a loss process characterized by a rate constant.

As a third application, Donley *et al.* [29] have conducted an experiment where two trapezoidal pulses in the magnetic field were applied. As a function of the time between the two pulses an oscillatory behavior in the number of condensate atoms is observed, which is attributed to coherent Rabi oscillations between atoms and molecules [30–32]. In this paper, we will not consider this experiment, but instead focus on the first and second experimental applications. In particular, the single-pulse experiment has not received much attention theoretically, even though an understanding of this experiment seems an essential first step in the theoretical treatment of the recent two-pulse experiment. Therefore, the discussion of this most recent experiment will be postponed to a future publication.

In a previous paper, we have considered the loss of atoms by means of elastic two-body collisions, in the situation where the condensate collapses [34]. However, the mechanism put forward in this paper is much more general. In particular, the mechanism should also be relevant for the above-mentioned single-pulse experiments. The main goal of this paper is to present the theory behind it in great detail. Since the mechanism is able to describe loss from a condensate at zero temperature, we will hereafter refer to it as quantum evaporation. The two-pulse experiments of Donley *et al.* [29] have made it clear that atom-molecule coherence can have an important effect on the dynamics of a Bose-Einstein condensate. Besides the quantum evaporation process, we thus want to consider this physics in the case of the single-pulse experiments as well. We are able to achieve this because very recently we have derived an effective quantum field theory that offers a description of the Feshbach resonance in terms of an atom-molecule Hamiltonian, that captures all the relevant two-body physics exactly [28]. Apart from a detailed discussion of the condensate collapse, the main application of this paper therefore concerns the effect of quantum evaporation in the single-pulse experiments and the investigation of the importance of atom-molecule coherence in this case. With respect to the latter remark it should be noted that the effect of atom-molecule coherence in the case of the condensate collapse will be neglected in the following, because the magnetic field is tuned to a far off-resonant value to induce the collapse.

In view of this, the paper is organized as follows. In Sec. II, we present and discuss the theoretical description of quantum evaporation. In Sec. III, we present the applications to the condensate collapse, and to the single-pulse experiments with positive scattering length. We end in Sec. IV with our conclusions.

II. QUANTUM EVAPORATION

In this section, we derive the generalized Gross-Pitaevskii equation that includes the correction term due to the quantum evaporation of atoms out of the condensate. From this result follows a rate equation for the change in the number of atoms in the condensate. Section II A is rather technical and may be omitted in a first reading. To facilitate this the final rate equation, which is most important for our purposes, is presented in Sec. II B.

A. Generalized Gross-Pitaevskii equation

Although the desired rate equation for the number of atoms can also be derived from the imaginary-time formalism by means of a Wick rotation to real time, the equation of motion for the condensate wave function cannot be derived in this manner. Therefore, we use a functional formulation of the Schwinger-Keldysh nonequilibrium theory [35,36] developed in Refs. [37–39], from which the equation of motion for the condensate wave function follows directly as the equation for the ''classical'' part of the fluctuating order-parameter field.

Within this formalism, the Wigner probability distribution of the order parameter is written as a functional integral over complex fields $\psi^*(\mathbf{x},t)$ and $\psi(\mathbf{x},t)$. These fields are defined on the Keldysh contour $\mathcal{C}^t$, which runs from t_0 to t and then back to t_0. The probability distribution is given by

$$P[\phi^*,\phi;t]=\int_{\psi^*(\mathbf{x},t)=\phi^*(\mathbf{x})}^{\psi(\mathbf{x},t)=\phi(\mathbf{x})} d[\psi^*]d[\psi]\exp\left\{\frac{i}{\hbar}S[\psi^*,\psi]\right\}, \tag{2}$$

where we absorbed the appropriate initial condition $P[\phi^*,\phi;t_0]$ into the measure of the functional integral [39]. The action in the exponent of the integrand is given by

$$S[\psi^*,\psi]=\int_{\mathcal{C}^t}dt'\int d\mathbf{x}'\,\psi^*(\mathbf{x}',t')\left[i\hbar\frac{\partial}{\partial t'}+\frac{\hbar^2\nabla^2}{2m}-V^{\mathrm{ext}}(\mathbf{x}')-\frac{T^{2\mathrm{B}}(t')}{2}|\psi(\mathbf{x}',t')|^2\right]\psi(\mathbf{x}',t'), \tag{3}$$

where $V^{\mathrm{ext}}(\mathbf{x})$ is the external trapping potential. The interaction is determined by the two-body T (transition) matrix element $T^{2\mathrm{B}}(t)=4\pi a(t)\hbar^2/m$, where $a(t)\equiv a((B(t))$ is the interatomic s-wave scattering length, and m is the mass of one atom. Note that we explicitly allowed the scattering length to depend on time. This is experimentally realized by tuning the magnetic field near the Feshbach resonance.

To arrive at an effective action for the condensate wave function, we explicitly separate out the condensate part from the field $\psi(\mathbf{x},t)$. Therefore, we write $\psi(\mathbf{x},t)=\psi_0(\mathbf{x},t)+\psi'(\mathbf{x},t)$, and substitute this into the action in Eq. (3). In this separation, $\psi_0(\mathbf{x},t)$ describes the condensed part of the gas, whereas $\psi'(\mathbf{x},t)$ describes the fluctuations. The precise distinction between the condensate and the noncondensed part is discussed in detail in Sec. III. Physically, the idea is that $\psi_0(\mathbf{x},t)$ describes the Bose-Einstein condensate and its collective modes, whereas $\psi'(\mathbf{x},t)$ is associated with the modes not occupied by the condensate. To define these two parts consistently, we have to require that they are essentially orthogonal, i.e.,

$$\int d\mathbf{x}[\psi_0^*(\mathbf{x},t)\psi'(\mathbf{x},t)+\psi'^*(\mathbf{x},t)\psi_0(\mathbf{x},t)]=0. \tag{4}$$

This condition ensures that the Jacobian of the transformation of integration variables in the functional integral in Eq. (2) is equal to 1. In the operator formalism, this condition implies that the Bose field operators $\hat{\psi}'(\mathbf{x},t)$ and $\hat{\psi}'^{\dagger}(\mathbf{x},t)$ associated with the fluctuations, obey the usual Bose commutation relations in the Fock space built upon the states orthogonal to $\psi_0(\mathbf{x},t)$.

After this substitution, the functional integral becomes

$$P[\phi^*,\phi;t]=\int d[\psi_0^*]d[\psi_0]\exp\left\{\frac{i}{\hbar}S[\psi_0^*,\psi_0]\right\}\times\int d[\psi'^*]d[\psi']\exp\left\{\frac{i}{\hbar}S_{\mathrm{int}}[\psi_0^*,\psi_0,\psi'^*,\psi']+\frac{i}{\hbar}S'[\psi_0^*,\psi_0,\psi'^*,\psi']\right\}. \tag{5}$$

Here, we define $S'[\psi_0^*,\psi_0,\psi'^*,\psi']$ such that it contains the terms up to quadratic order in the fluctuations. We do not retain the terms proportional to $(\psi')^2$ and $(\psi'^*)^2$, since these so-called anomalous terms are only needed to describe the collective motion of the condensate. Their effect is, therefore, already included in the action $S[\psi_0^*,\psi_0]$ for the part of the field that describes the condensate. In principle, $S_{\mathrm{int}}[\psi_0^*,\psi_0,\psi'^*,\psi']$ contains terms which are either of first, third, or fourth order in the fluctuations. We neglect, however, the terms of third and fourth order, which is known as the Bogoliubov approximation. This approximation is valid for the zero-temperature applications under consideration in this paper. Moreover, the terms of higher order in the fluctuations describe the interactions among the ejected atoms and are expected to be of little importance in determining the ejection rate for the atoms expelled from the condensate.

We write the quadratic action $S'[\psi_0^*,\psi_0,\psi'^*,\psi']$ as

$$S'[\psi_0^*,\psi_0,\psi'^*,\psi']=\int_{\mathcal{C}^t}dt'\int d\mathbf{x}'\int_{\mathcal{C}^t}dt''\int d\mathbf{x}''\psi'^*(\mathbf{x}',t')\times\hbar G^{-1}(\mathbf{x}',t';\mathbf{x}'',t'')\psi'(\mathbf{x}'',t''), \tag{6}$$

where we introduced the Green's function $G(\mathbf{x},t,\mathbf{x}',t')$ for the fluctuations by means of

$$\left[i\hbar\frac{\partial}{\partial t}+\frac{\hbar^2\nabla^2}{2m}-V^{\mathrm{ext}}(\mathbf{x})-2T^{2\mathrm{B}}(t)|\psi_0(\mathbf{x},t)|^2\right]G(\mathbf{x},t,\mathbf{x}',t')=\hbar\delta(\mathbf{x}-\mathbf{x}')\delta(t,t'). \tag{7}$$

Here, the δ function in the time variables is defined on the Keldysh contour, by means of $\int_{\mathcal{C}^t}dt'\,\delta(t,t')=1$. The part of the action that describes the interactions between the condensed and noncondensed parts of the system is, in first instance, given by

$$S_{\mathrm{int}}[\psi_0^*,\psi_0,\psi'^*,\psi']=\int_{\mathcal{C}^t}dt'\int d\mathbf{x}'\left\{\psi_0^*(\mathbf{x}',t')\left[i\hbar\frac{\partial}{\partial t'}+\frac{\hbar^2\nabla^2}{2m}-V^{\mathrm{ext}}(\mathbf{x}')-T^{2\mathrm{B}}(t')|\psi_0(\mathbf{x}',t')|^2\right]\psi'(\mathbf{x}',t')+\psi'^*(\mathbf{x}',t')\left[i\hbar\frac{\partial}{\partial t'}+\frac{\hbar^2\nabla^2}{2m}-V^{\mathrm{ext}}(\mathbf{x}')-T^{2\mathrm{B}}(t')|\psi_0(\mathbf{x}',t')|^2\right]\psi_0(\mathbf{x}',t')\right\}. \tag{8}$$

It is important to note that this part of the action does not vanish because the condensate wave function, as we see in a moment, does not obey the usual Gross-Pitaevskii equation once we include the quantum evaporation process. Furthermore, the field $\psi'(\mathbf{x},t)$ describes the high-energy part of the system, and thus has an expansion in terms of the high-energy trap states. As a result, we are allowed to neglect the terms proportional to the single-particle Hamiltonian. The terms with the time derivative vanish because of the orthogonality condition in Eq. (4). The action in Eq. (8), therefore, reduces to

$$S_{\mathrm{int}}[\psi_0^*,\psi_0,\psi'^*,\psi']=-\int_{\mathcal{C}^t}dt'\int d\mathbf{x}'[J^*(\mathbf{x}',t')\psi'(\mathbf{x}',t')+\psi'^*(\mathbf{x}',t')J(\mathbf{x}',t')], \tag{9}$$

where we introduced the ''current density''

$$J(\mathbf{x},t)=T^{2\mathrm{B}}(t)|\psi_0(\mathbf{x},t)|^2\psi_0(\mathbf{x},t). \tag{10}$$

The functional integral over the fluctuations in Eq. (5) is a Gaussian integral and can be easily performed. This defines the effective action for the condensate on the Keldysh contour by means of

$$\begin{aligned}P[\phi^*,\phi;t]=&\int d[\psi_0^*]d[\psi_0]\exp\left\{\frac{i}{\hbar}S[\psi_0^*,\psi_0]\right\}\\&\times\int d[\psi'^*]d[\psi']\exp\left\{\frac{i}{\hbar}S_{\mathrm{int}}[\psi_0^*,\psi_0,\psi'^*,\psi']\right.\\&\left.+\frac{i}{\hbar}S'[\psi_0^*,\psi_0,\psi'^*,\psi']\right\}\\\equiv&\int d[\psi_0^*]d[\psi_0]\exp\left\{\frac{i}{\hbar}S_{\mathrm{eff}}[\psi_0^*,\psi_0]\right\},\end{aligned} \tag{11}$$

and results in

$$\begin{aligned}S_{\mathrm{eff}}[\psi_0^*,\psi_0]=&S[\psi_0^*,\psi_0]-\frac{1}{\hbar}\int_{\mathcal{C}^t}dt'\int d\mathbf{x}'\int_{\mathcal{C}^t}dt''\int d\mathbf{x}''\\&\times J^*(\mathbf{x}',t')G(\mathbf{x}',t';\mathbf{x}'',t'')J(\mathbf{x}'',t'').\end{aligned} \tag{12}$$

Because the Green's function in this effective action is equal to

$$iG(\mathbf{x}',t';\mathbf{x}'',t'')\equiv\mathrm{Tr}\{\hat{\rho}(t_0)T_{\mathcal{C}^t}(\hat{\psi}'(\mathbf{x}',t')\hat{\psi}'^{\dagger}(\mathbf{x}'',t''))\}_{J=0}, \tag{13}$$

where $T_{\mathcal{C}^t}$ denotes time ordering along the Keldysh contour and $\hat{\rho}(t_0)$ represents the initial density matrix of the gas, this Green's function can be decomposed into its analytic pieces by means of

$$\begin{aligned}G(\mathbf{x},t;\mathbf{x}',t')=&\theta(t,t')G^{>}(\mathbf{x},t;\mathbf{x}',t')\\&+\theta(t',t)G^{<}(\mathbf{x},t;\mathbf{x}',t'),\end{aligned} \tag{14}$$

with $\theta(t,t')$ the Heaviside function on the Keldysh contour. The Green's functions $G^{>}$ and $G^{<}$ thus correspond to averages of a fixed order of creation and annihilation operators. Note that these Green's functions essentially describe the propagation of a noncondensed atom in the presence of the mean-field interaction with the condensate.

To finally derive the generalized Gross-Pitaevskii equation for the condensate wave function, we want to separate out the classical part of the field $\psi_0(\mathbf{x},t)$. This is achieved by means of the transformation

$$\psi_0(\mathbf{x},t_{\pm})=\phi(\mathbf{x},t)\pm\frac{\xi(\mathbf{x},t)}{2}, \tag{15}$$

where the upper (lower) sign corresponds to the forward (backward) branch of the Keldysh contour. Here, $\phi(\mathbf{x},t)$ denotes the condensate wave function, whereas the field $\xi(\mathbf{x},t)$ describes its quantum and thermal fluctuations. From a fundamental point of view, the latter field together with an appropriate fluctuation-dissipation theorem ensures that in equilibrium the occupation numbers of the Bose-Einstein condensate and its collective modes are given by the Bose distribution function [39]. When substituting this transformation into the effective action in Eq. (12), we should, in principle, only keep terms up to quadratic order in the fluctuations, to avoid a double counting of the interactions that we have already taken into account. However, to read off the generalized Gross-Pitaevskii equation, including the correction terms associated with the quantum evaporation process, it suffices to consider only the linear terms in the fluctuations. This can be understood from the fact that with this approximation a functional integration over the fluctuations leads to a constraint for $\phi(\mathbf{x},t)$, which is precisely the classical equation of motion that we are interested in. With the transformation in Eq. (15), we thus project the effective action on the real-time axis and read off the equations of motion for $\phi(\mathbf{x},t)$ and $\phi^*(\mathbf{x},t)$ by putting the coefficient of the terms linear in $\xi^*(\mathbf{x},t)$ and $\xi(\mathbf{x},t)$ equal to zero, respectively. After straightforward but somewhat tedious algebra, this results in

$$\begin{aligned}i\hbar\frac{\partial\phi(\mathbf{x},t)}{\partial t}=&\left[-\frac{\hbar^2\nabla^2}{2m}+V^{\mathrm{ext}}(\mathbf{x})+T^{2\mathrm{B}}(t)|\phi(\mathbf{x},t)|^2\right]\phi(\mathbf{x},t)\\&+\left\{\frac{T^{2\mathrm{B}}(t)}{\hbar}\int_{-\infty}^{\infty}dt'\int d\mathbf{x}'\,T^{2\mathrm{B}}(t')\right.\\&\times[2\phi^*(\mathbf{x},t)G^{(+)}(\mathbf{x},t;\mathbf{x}',t')\phi(\mathbf{x}',t')\\&+\phi(\mathbf{x},t)G^{(-)}(\mathbf{x}',t';\mathbf{x},t)\phi^*(\mathbf{x}',t')]\\&\left.\times|\phi(\mathbf{x}',t')|^2\right\}\phi(\mathbf{x},t)\end{aligned} \tag{16}$$

with the complex conjugate expression for $\phi^*(\mathbf{x},t)$. We defined the retarded and the advanced Green's functions in the usual way by

$$\begin{aligned}G^{(\pm)}(\mathbf{x},t;\mathbf{x}',t')=&\pm\theta(\pm(t-t'))[G^{>}(\mathbf{x},t;\mathbf{x}',t')\\&-G^{<}(\mathbf{x},t;\mathbf{x}',t')].\end{aligned} \tag{17}$$

Note that the Heaviside function in this definition is precisely such that the equation of motion for $\phi(\mathbf{x},t)$ is causal.

The time-ordered Feynman diagrams corresponding to the two terms in the generalized Gross-Pitaevskii equation describing the quantum evaporation process are given in Figs. 2(a) and 2(b), respectively. In these diagrams, a condensate atom is denoted by a dashed line. An ingoing dashed line thus corresponds to a factor $\phi(\mathbf{x},t)$, and an outgoing dashed line to a factor $\phi^*(\mathbf{x},t)$. The advanced and retarded propagators of the ejected atoms are denoted by solid lines. A retarded propagator is denoted by an arrow pointing from $(\mathbf{x}',t')$ to $(\mathbf{x},t)$, and corresponds to the propagation of a particle. An advanced propagator is denoted by a reversed arrow, and can be interpreted as the propagation of a ''hole.'' Note that the first term in Eq. (16) has an additional factor of 2 with respect to the second term. This is understood from

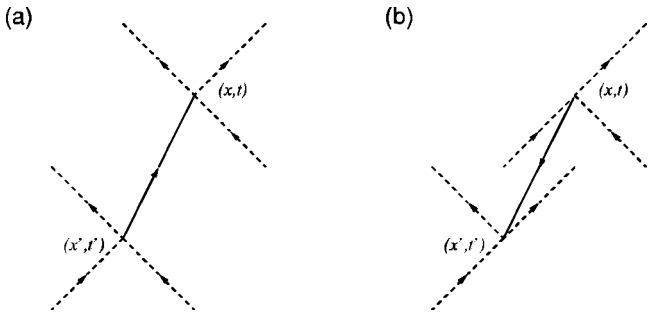

FIG. 2. These time-ordered Feynmans diagrams correspond to terms associated with quantum evaporation in the equation of motion for the condensate wave function.

the fact that the corresponding diagram [Fig. 2(a)] has two outgoing lines at $(\mathbf{x},t)$ and therefore contributes twice, whereas the diagram in Fig. 2(b) has only one outgoing line at those coordinates.

B. Rate equation

In the preceding section, we have generalized the Gross-Pitaevskii equation to include the quantum evaporation process. With this equation, we derive a rate equation for the number of atoms in the condensate. It is given by

$$\frac{dN_c(t)}{dt}=\frac{d}{dt}\int d\mathbf{x}|\phi(\mathbf{x},t)|^2$$
$$=\frac{2}{\hbar^2}\int d\mathbf{x}\int_{-\infty}^{\infty}dt'\int d\mathbf{x}'\,\mathrm{Im}[T^{2B}(t)|\phi(\mathbf{x},t)|^2$$
$$\times\phi^*(\mathbf{x},t)G^{(+)}(\mathbf{x},t;\mathbf{x}',t')T^{2B}(t')$$
$$\times|\phi(\mathbf{x}',t')|^2\phi(\mathbf{x}',t')]. \tag{18}$$

The retarded propagator $G^{(+)}(\mathbf{x},t;\mathbf{x}',t')$ describes the noncondensed atoms. Note that in both, this rate equation and the equation of motion in Eq. (16) we have taken the limit $t_0\to-\infty$ to eliminate initial transient effects. Furthermore, we have made use of the fact that $[G^{(+)}(\mathbf{x},t;\mathbf{x}',t')]^*=G^{(-)}(\mathbf{x}',t';\mathbf{x},t)$, which follows from the definition of this Green's function.

The non-Markovian rate equation in Eq. (18) describes the evolution of the number of condensate atoms due to a change in the scattering length or the condensate wave function. Physically, the coupling between the condensed and noncondensed parts of the system allows the condensate to eject atoms. Since we have neglected the interactions among the ejected atoms, this rate equation is applicable only for short times and does not describe the rethermalization of the ejected atoms. Because of this approximation, the ejection process is coherent, and atoms can come back into the condensate on short-time scales. To get more physical insight into the quantum evaporation process, we discuss the weak-coupling limit, where it just corresponds to elastic condensate collisions.

In the weak-coupling limit, where the mean-field interaction is small compared to the energy-level splitting of the external trapping potential, the rate equation for the number of atoms in the condensate acquires a familiar form. To see this, we note that in this limit the retarded propagator is given by

$$G^{(+)}(\mathbf{x},t;\mathbf{x}',t')=-i\theta(t-t')\sum_{\mathbf{n}\neq0}e^{-(i/\hbar)\epsilon_{\mathbf{n}}(t-t')}$$
$$\times\chi_{\mathbf{n}}(\mathbf{x})\chi_{\mathbf{n}}^*(\mathbf{x}'), \tag{19}$$

because the single-particle states $\chi_{\mathbf{n}}(\mathbf{x})$ and energies $\epsilon_{\mathbf{n}}$ are, in this limit, by definition not affected much by the interactions. The sum in this expression is over all the trap states, except for the condensate mode, i.e., the one-particle ground state.

The condensate wave function is given by

$$\phi(\mathbf{x},t)=e^{-(i/\hbar)\mu t}\sqrt{N_c(t)}\chi_0(\mathbf{x}), \tag{20}$$

where $\mu\equiv\epsilon_0$ is the ground-state energy, and $N_c\gg1$ is the number of atoms in the condensate. Using these expressions, the rate equation for the number of atoms in Eq. (18) can be rewritten as

$$\frac{dN_c(t)}{dt}=-\left[\frac{N_c^3(t)}{2}\right]\frac{2\pi}{\hbar}\sum_{\mathbf{n}\neq0}\delta(\epsilon_{\mathbf{n}}-\epsilon_0)|\langle\mathbf{n}|\hat{V}|0\rangle|^2, \tag{21}$$

which is precisely Fermi's golden rule for the rate to scatter out of the initial state $|0\rangle$, found from second-order perturbation theory. The sum is over all final states of the form

$$\langle\mathbf{x}_1\mathbf{x}_2|\mathbf{n}\rangle\equiv\frac{1}{\sqrt{2}}[\chi_0(\mathbf{x}_1)\chi_{\mathbf{n}}(\mathbf{x}_2)+\chi_{\mathbf{n}}(\mathbf{x}_1)\chi_0(\mathbf{x}_2)], \tag{22}$$

with energy $\epsilon_{\mathbf{n}}+\mu$. Since we are dealing with identical bosons, these states are symmetric. This final state thus represents a condensate atom and an ejected atom, whereas the initial state with energy 2μ is given by

$$\langle\mathbf{x}_1\mathbf{x}_2|0\rangle\equiv\chi_0(\mathbf{x}_1)\chi_0(\mathbf{x}_2), \tag{23}$$

and therefore represents two condensate atoms. The additional factor N_c^3 is a result of the Bose statistics of the atoms. There is a factor $N_c(N_c-1)/2\approx N_c^2/2$ for the number of condensate atom pairs and an additional factor $1+N_c\approx N_c$ for the condensate atom that is Bose stimulated back into the condensate. Finally, the potential is given by

$$\hat{V}=T^{2B}\delta(\hat{\mathbf{x}}_1-\hat{\mathbf{x}}_2). \tag{24}$$

We see that, in the weak-coupling limit, the energy-conserving δ function can never be obeyed, and thus $dN_c/dt=0$, as expected in this limit. Another important observation is that energy conservation also forbids the ejection of atoms out of a static condensate with repulsive interactions, even in the strong-coupling limit. This is because of the fact that the energy of a condensate atom, i.e., the chemical potential, is positive in this case, and that the energy of the excited states is always larger than the chemical poten-

tial. This leads to the important conclusion that in order to eject atoms out of the condensate by means of the quantum evaporation process, there has to be a strong time dependence of either the condensate wave function, or of the scattering length. In the following section, we discuss two experimentally relevant examples where this is the case.

III. APPLICATIONS

In this section we apply the theory, described in the previous section, to two different experimental situations. In the first part, we consider the case where the Feshbach resonance is used to investigate the collapse of a condensate [9,21]. In the second part, we apply our theory to the situation where the scattering length is changed very rapidly back and forth from zero to a large and positive value [33]. We also discuss the importance of atom-molecule coherence in this case.

A. Condensate collapse

The use of a Feshbach resonance has made it possible to explore the physics of the collapse in two different regimes. First, we can have a collapse in which the dynamics of the condensate is mostly determined by the mean-field interactions. This is the case in the experiments with ^{7}Li [15–17,19], which has a fixed negative scattering length. In these experiments, there is always a large thermal component which feeds the condensate. Therefore, we call such a collapse a type-I collapse, in analogy with a type-I supernova, which is believed to be the result of an accreting white dwarf that explodes when the accumulated mass becomes large [51], similar to the ^{7}Li condensate that grows from the thermal cloud and then collapses. The more recent experiments by Donley *et al.* [21] also deal with a type-I collapse, since one starts a collapse from the noninteracting limit, where the density is relatively high compared to Bose-Einstein condensates with a repulsive self-interaction.

Complementary to this regime we can have a second type of collapse where the dynamics is mostly determined by the external trapping potential. This regime was considered experimentally by Cornish *et al.* [9]. Using the Feshbach resonance of ^{85}Rb at $B_0 \approx 154.9$ G, one first makes a large, stable, and essentially pure condensate, i.e., there is no visible thermal cloud present, with repulsive interactions. Then, one suddenly switches the interactions from repulsive to slightly attractive, and watches the subsequent collapse. Because the collapse in this case starts at low density due to the initially large and repulsive interatomic interactions and the magnitude of the final negative scattering length is much smaller than the initial positive one, its dynamics is mostly determined by the trapping potential. We call such a collapse a type-II collapse, in analogy with a type-II supernova. Such a supernova is the fate of a massive star analogous to the large condensate with repulsive interactions.

In the experiments on the type-II collapse, it was found that after such a collapse the number of atoms in the condensate is of the same order as the maximum number of atoms allowed to have a metastable condensate [40]. This suggests that during such a collapse, enough atoms are ejected from the condensate, so that the condensate becomes metastable. The most important theoretical task is therefore to identify the physical mechanism responsible for this ejection. We have recently argued that the quantum evaporation process provides an explanation for these experiments [34]. Moreover, we will explicitly show here that the decay solely by means of three-body recombination does not explain the experimental results for the type-II collapse.

Interestingly, the metastable condensate that is the result of a type-II collapse is precisely the starting point for a type-I collapse, making this last collapse a much more violent phenomenon. We restrict ourselves here to the description of the type-II collapse, because a proper treatment of the type-I collapse requires a full numerical solution of the generalized Gross-Pitaevskii equation that includes the nonlocal correction term due to quantum evaporation. This is beyond the scope of the present paper, and we use a simpler variational approach here that we believe is appropriate for a type-II-collapse event.

1. Gaussian approximation and semiclassical retarded propagator

In principle, we must now numerically solve the generalized Gross-Pitaevskii equation in Eq. (16) that includes nonlocal terms. However, in order to gain physical insight, we will make several approximations to reduce the solution of this equation to a numerically more tractable problem. First of all, we use a Gaussian variational approach to the condensate wave function [52]. More precisely, we assume the condensate wave function to be of the form

$$\phi(\mathbf{x},t) = \sqrt{N_c(t)}\, e^{i\theta_0(t)} \prod_j \left(\frac{1}{\pi q_j^2(t)} \right)^{1/4} \times \exp\left\{ -\frac{x_j^2}{2q_j^2(t)} \left(1 - i \frac{m q_j(t)}{\hbar} \frac{dq_j(t)}{dt} \right) \right\}. \quad (25)$$

In the limit of a small number of condensate atoms $N_c(t)$, this ansatz becomes an exact solution of the Gross-Pitaevskii equation for a harmonic external trapping potential, and therefore a good description of the condensate after the collapse. It is, however, also known that a Gaussian ansatz gives good results on the frequencies of the collective modes, even in the Thomas-Fermi regime [41]. Moreover, since we consider only the type-II collapse and therefore by definition assume that the trapping potential is more important than the mean-field interactions, we expect the Gaussian ansatz to give physically reasonable results at all times.

In the case of the ordinary Gross-Pitaevskii equation the variational parameters obey Newton's equation of motion [12]

$$m \frac{d^2 q_j(t)}{dt^2} = -\frac{\partial}{\partial q_j} V(\mathbf{q}(t); N_c(t)), \quad (26)$$

with a potential given by

$$V(\mathbf{q};N_c)=\sum_j\left(\frac{\hbar^2}{2mq_j^2}+\frac{m\omega_j^2q_j^2}{2}\right)+\sqrt{\frac{2}{\pi}}\frac{a(t)\hbar^2N_c}{mq_xq_yq_z}, \tag{27}$$

where the frequencies ω_j are the frequencies of the harmonic external trapping potential in the three spatial directions. We have recently extended the above variational calculus also to the case of a nonlinear Schrödinger equation including an imaginary term due to the presence of a thermal cloud, and found that the equation of motion for the variational parameters, in principle, contains a damping term [18]. However, we are interested in the zero-temperature situation, in which this damping term is negligible. This means that for a description of the collapse, we only have to couple Eq. (26) to the rate equation for the number of atoms in Eq. (18).

To determine this rate equation in detail, we need an expression for the propagator of the ejected atoms. Anticipating that the energy of the ejected atoms will be much higher than the energy of a condensate atom, we take for the one-particle Green's function of the ejected atoms the semiclassical approximation

$$G^{(+)}(\mathbf{x},t;\mathbf{x}',t')=-i\,\theta(t-t')\int\frac{d\mathbf{k}}{(2\pi)^3}\times e^{-(i/\hbar)\epsilon(\mathbf{k},\mathbf{R},T)(t-t')}e^{i\mathbf{k}\cdot(\mathbf{x}-\mathbf{x}')}, \tag{28}$$

where we introduced the center-of-mass coordinate $\mathbf{R}=(\mathbf{x}+\mathbf{x}')/2$, and used $T=(t+t')/2$ for notational convenience. The energy of the ejected atoms is, in this approximation, given by

$$\epsilon(\mathbf{k},\mathbf{R},T)=\frac{\hbar^2\mathbf{k}^2}{2m}+V^{\mathrm{ext}}(\mathbf{R})+2T^{2B}(T)|\phi(\mathbf{R},T)|^2+\epsilon_1. \tag{29}$$

This energy is measured from ϵ_1, which is the first excited level in the trap. This energy thus determines the cutoff between the condensate and the ejected atoms. Although this cutoff is important to make the distinction between condensate and noncondensate atoms, we find that our numerical results are not very sensitive to its precise value.

Since the most important contribution to the rate equation comes from the center of the trap, we expect that we can, to a good approximation, take for the energy of an ejected atom the value $\epsilon(\mathbf{k},\mathbf{0},T)\equiv\epsilon(\mathbf{k},T)$. We use this value for the energy of an ejected atom from now on. This approximation is very convenient, since we can now perform the spatial integrals in the rate equation, as well as the integral over the momenta in the expression for the retarded propagator analytically. The final result is given in Appendix A.

In the ansatz in Eq. (25), we have included a global phase $\theta_0(t)$. This is important, since we have already seen in the preceding section that this global phase determines the energy of a condensate atom in equilibrium. We can determine this global phase by insertion of the ansatz in the Gross-Pitaevskii equation including the correction term in Eq. (16), and separating out the real part. Neglecting the contribution of the quantum evaporation process to the mean-field energy, it is up to an irrelevant constant given by [18]

$$\theta_0(t)=-\frac{1}{\hbar}\left\{\int_{-\infty}^{t}d\tau\left[\frac{\partial V(\mathbf{q}(\tau),N_c(\tau))}{\partial N_c}-\sum_j\frac{1}{4}m\dot{q}_j^2(\tau)\right]+\sum_j\frac{1}{4}mq_j(t)\dot{q}_j(t)\right\}. \tag{30}$$

Note that in equilibrium, this results in a phase factor $e^{-i\mu t/\hbar}$ for the condensate wave function, with $\mu=\partial V(\mathbf{q},N_c)/\partial N_c$. This is clearly the correct expression for the chemical potential.

With the above approximations, we have reduced the difficult problem of solving a partial differential equation with a nonlocal correction term to the problem of solving the ordinary differential equations for the variational parameters in Eq. (26) coupled to the rate equation for the change in the number of atoms in Eq. (18). This rate equation is now only nonlocal in time, since all the integrals can be done analytically for the Gaussian wave function and the semiclassical retarded propagator we are considering here. In the following section, we will present our results obtained by numerically solving these equations.

2. Results

We have performed numerical simulations for the experimental conditions of Cornish *et al.* [9,40] with ^{85}Rb. The frequencies of the external trapping potential are equal to $\omega_r/2\pi=17.4$ Hz and $\omega_z/2\pi=6.8$ Hz, in the radial and axial directions, respectively. One starts with a condensate consisting of $N_c(0)\approx4000$ atoms and a scattering length of $a(B_i)=2500a_0$, where B_i is the magnetic field at the initial time. Initially, there is no visible thermal cloud present, so the system is approximately at zero temperature. One then ramps the magnetic field linearly in a time Δt from its initial value B_i to the final value B_f, chosen such that $a(B_f)=-60a_0$. The ramp time is taken equal to $\Delta t=0.5$ ms.

To investigate the importance of three-body recombination during the collapse, we have included it in our simulations in addition to the quantum evaporation process. This amounts to including a term

$$-\frac{i\hbar}{2}\frac{K_3}{3!}|\phi(\mathbf{x},t)|^4\phi(\mathbf{x},t)$$

on the right-hand side of Eq. (16), from which the contribution to the rate equation for the number of atoms can be easily found. Although there are several predictions for the normal-component rate constant K_3 [42–45], its behavior as a function of the magnetic field is unknown near the Feshbach resonance and precise experimental data are unavailable [47]. Following Saito and Ueda [26], we take $K_3=1.2\times10^{-27}$ cm^6/s. With this value, these authors have been able to explain some of the results of the experiment on the type-I collapse by Donley *et al.* [21]. Since the final value of the magnetic field is in the same range for both experiments, we expect the three-body recombination rate constant to be of the same order of magnitude.

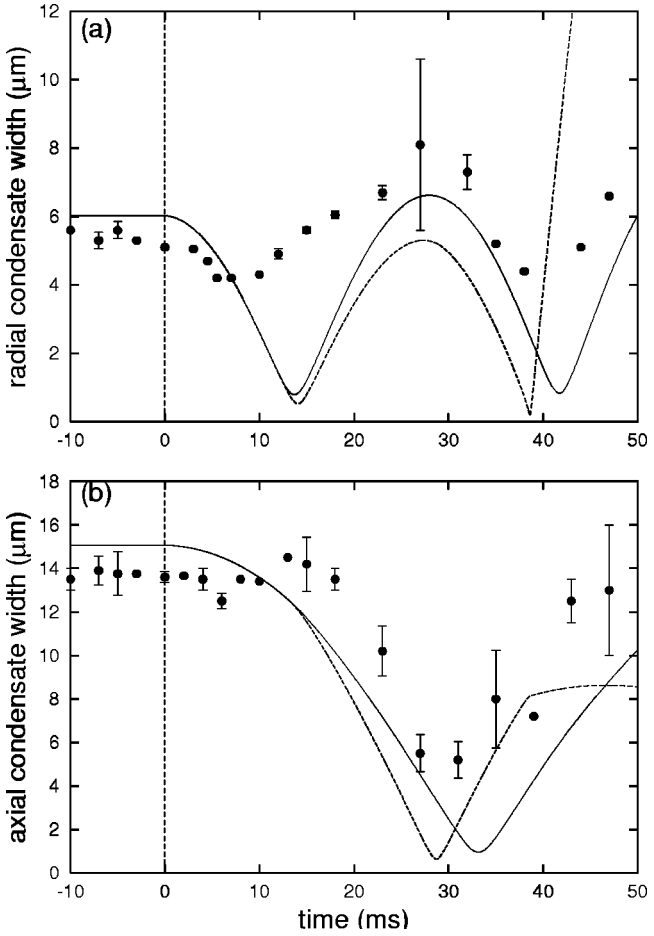

FIG. 3. (a) Radial and (b) axial width of the condensate as a function of time during a type-II collapse. At the origin of the time axis, the scattering length vanishes as it is changed from large and postive to negative. The solid line corresponds to a simulation where both quantum evaporation and three-body recombination are included. The dashed line corresponds to a simulation including only three-body recombination. The experimental points are also shown and taken from Ref. [40].

In Figs. 3 and 4, we present the results of our simulations. The widths of the condensate in the radial and axial directions, i.e., the variational parameters q_r and q_z, are shown as a function of time in Figs. 3(a) and 3(b), respectively. The number of atoms as a function of time is displayed in Fig. 4. The origin of the time axis is chosen such that the scattering length is equal to zero at $t=0$. The solid line corresponds to a simulation that includes both the quantum evaporation process and three-body recombination. The condensate collapses first in the radial direction in a time $\pi/(2\omega_r)\approx 14$ ms and during the last part of this radial collapse the condensate ejects a large fraction of its atoms, by means of the quantum evaporation process. In our simulations, we find that the three-body recombination hardly contributes. After a time $\pi/(2\omega_z)\approx 36$ ms the axial width of the condensate reaches its minimum, resulting again in a slight increase of the ejection rate. Note that these time scales are expected, since the dynamics is determined by the external trapping potential. More remarkably, for a very short time the number of atoms

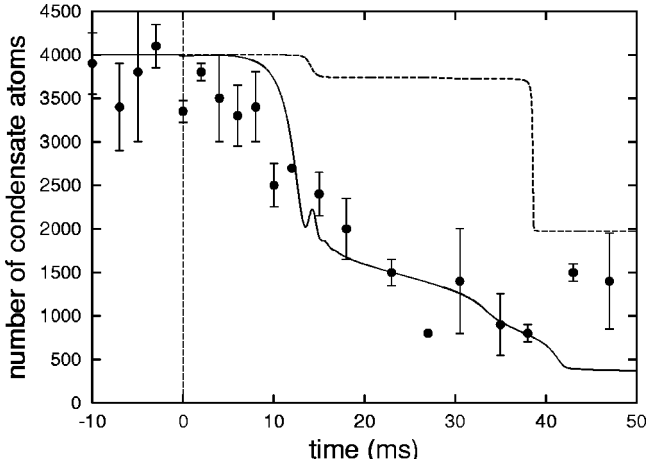

FIG. 4. Number of atoms in the condensate as a function of time during a type-II collapse. The solid line corresponds to a simulation where both quantum evaporation and three-body recombination are included. The dashed line corresponds to a simulation including only three-body recombination. The experimental points are also shown and taken from Ref. [40].

increases with time during the collapse. In principle, this can occur, because the quantum evaporation process is coherent, and can thus describe multimode Rabi oscillations between the condensate and the noncondensed part of the system, as we shall see in much more detail in the following section.

The simulation that includes the quantum evaporation process shows quantitative agreement with the experimental results [40], which are also shown in Figs. 3 and 4. The disagreement for small values of the widths of the condensate is a result of the fact that the experimental resolution for the condensate size is about 4 μm [40].

We have also performed a simulation that includes only three-body recombination and no quantum evaporation. The results for this simulation are shown in Figs. 3 and 4 by the dashed lines. The fact that the minima in the widths of the condensate in Fig. 3 are lower than the results including quantum evaporation indicates that the condensate density has to be relatively high for the recombination of atoms to occur. Once such a high density is reached, the ejection of atoms occurs very fast, resulting in a staircaselike pattern for the number of atoms as a function of time, which is clearly not visible in the experimental data. At $t\approx 38$ ms the condensate decays so fast that the radial direction becomes stable again, resulting in a large increase of the radial width.

Finally, we make some remarks about the properties of the ejected atoms. In Ref. [34], we have calculated the distribution of the kinetic energy of the ejected atoms, as well as the angular distribution. We have also performed preliminary calculations of the average kinetic energy emitted in the radial and axial directions, and have found that the energy distribution of the ejected atoms is anisotropic. Donley *et al.* [21] have measured the angular and radial temperatures of the emitted atoms and have indeed found an anisotropic distribution of the energies. However, our calculations are done for the type-II collapse and our approximations are especially suited for this case, whereas these experiments deal with a type-I collapse. Therefore, we do not directly compare our

results with the available experimental data of Donley *et al.* [21]. Moreover, to improve the experimental resolution limit, one expands the gas at the end of each destructive measurement by an increase in the scattering length. Therefore, the resulting mean-field energy and rethermalization effects may play an important role in determining the energy of the ejected atoms, which is not included in our calculations of the energy distribution function in Ref. [34].

In conclusion, we have shown in this section that the simulations of the type-II collapse that include quantum evaporation show quantitative agreement with the experimental results. The most important feature of these experimental results is the fact that the condensate starts to eject atoms almost immediately after the initiation of the collapse. We have also shown that solely three-body recombination does not account for this rapid onset of the loss of atoms. At this point it is important to notice that this conclusion also holds if we numerically solve the generalized Gross-Pitaevskii equation, without approximations. The reason for this is that the Gaussian ansatz used here is certainly appropriate for the first part of the collapse, when the dynamics is not yet very violent. This is borne out by numerical simulations of the Gross-Pitaevskii equation, which have also shown that when the highest densities are reached during a type-I collapse, high-density ''spikes'' can form on the profile of the wave function [23–27]. These spikes are not included in our ansatz for the condensate wave function and therefore our approximations might be less appropriate for the highest densities reached during the collapse. However, our results suggest that such high-density spikes may well never occur if one includes the effects of the quantum evaporation process.

B. Multimode Rabi oscillations

Apart from the negative scattering length regime, the experimental control over the interatomic interactions has also made it possible to explore the regime where the interaction is large and positive. To this end, Claussen *et al.* [33] have conducted an experiment where the magnetic field undergoes a trapezoidal pulse in time, resulting in a quick jump in the scattering length towards a large positive value. In detail, one ramps the magnetic field linearly in a time t_{rise} from its value in the noninteracting limit ($B \approx 166.5$ G), to a value where the scattering is of the order of a few thousand Bohr radii. The magnetic field is kept at this value for a time t_{hold} before ramping back to the initial value again within the same t_{rise}. The scattering length as a function of time for a typical pulse is shown in Fig. 5 and the inset shows the corresponding magnetic field. The rise time t_{rise} and the hold time t_{hold} are typically of the order of 10–100 μs.

In this experiment, one observes particle loss from the condensate as a function of both the rise time and the hold time, accompanied by a ''burst'' of atoms from the condensate. The temperature of the burst atoms is of the same order as in the case of the experiments on the collapse, i.e., about 150 nK. Most importantly, the amount of atoms lost from the condensate decreases with increasing t_{rise} over some interval, which can never be the case for atom loss characterized by a rate constant, such as three-body recombination. Also note that the time scales of the pulse are very small compared to the time scales set by the inverse frequencies of the external trapping potential. This means that the density profile of the condensate hardly changes its shape during the pulse, since the collective modes which alter the density profile have frequencies of the same order of magnitude.

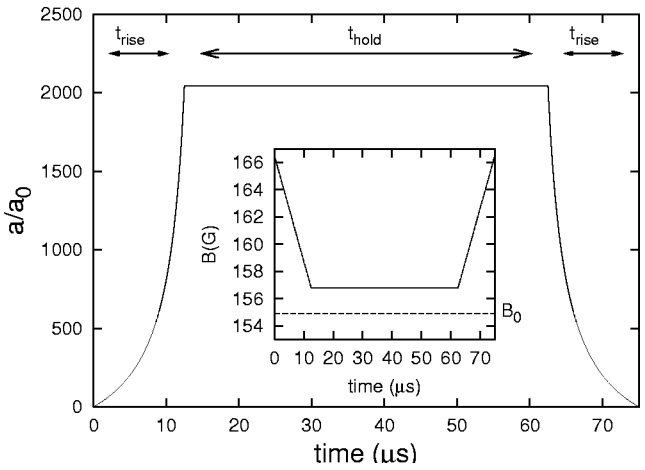

FIG. 5. The scattering length as a function of time in the experiments by Claussen *et al.* [33], and the corresponding magnetic field (inset). One increases the scattering length in a time t_{rise} by means of a linear ramp in the magnetic field, and holds the magnetic field for a time t_{hold}, before ramping back. The position of the Feshbach resonance is indicated by the dashed line.

1. Retarded propagator

The single-pulse experiments start in the noninteracting limit where the density profile of the condensate has the shape of a Gaussian, and the pulse in the magnetic field is so fast that the condensate wave function hardly changes due to the interactions. This makes it convenient to expand the propagator for the ejected atoms in the excited harmonic-oscillator eigenstates, since the condensate part is then left out most easily. The fact that the condensate density profile almost remains the shape of the ground state of the trap makes this problem easier to deal with theoretically and makes it therefore worthwhile to determine the propagator for the ejected atoms as accurate as possible. With the type-II-collapse problem of the preceding section, this objective is much more difficult, since then the condensate wave function changes its shape considerably during the collapse. This means that at each time a different number of trap states has to be included in the wave function, making the cutoff between condensate and noncondensed atoms strongly time dependent. Therefore, we have applied several approximations in that case. Even though the density profile of the condensate does not change much, the phase of the condensate wave function does change very fast in the single-pulse case. Therefore we use for the phase of condensate wave function the phase of the Gaussian ansatz given in Eq. (25). Since this wave function also describes the low-lying collective modes of the condensate, we have to exclude these from the propagator of the noncondensed atoms.

Denoting the eigenstates of the single-particle Hamiltonian again by $\chi_{\mathbf{n}}(\mathbf{x})$ and the corresponding eigenvalues by $\epsilon_{\mathbf{n}}$, we have for the propagator of the ejected atoms

$$G^{(+)}(\mathbf{x},t;\mathbf{x}',t') = -i\theta(t-t')\sum_{\mathbf{n},\mathbf{n}'}{}' a_{\mathbf{n},\mathbf{n}'}(t,t') \times \chi_{\mathbf{n}}(\mathbf{x})\chi^*_{\mathbf{n}'}(\mathbf{x}')e^{-(i/\hbar)(\epsilon_{\mathbf{n}}t-\epsilon_{\mathbf{n}'}t')}. \tag{31}$$

The prime denotes summation over all the excited trap states not contained in the condensate wave function. The equation of motion for the expansion coefficients $a_{\mathbf{n},\mathbf{n}'}(t,t')$ can be found by inserting Eq. (31) into the equation of motion for the Green's function given in Eq. (7). However, it is easier to realize that the Green's function is in Eq. (13) shown to be related to the expectation value of the product of two Heisenberg annihilation and creation operators for the noncondensed atoms. The equation of motion for the annihilation operator of interest is given by

$$\left[i\hbar\frac{\partial}{\partial t}+\frac{\hbar^2\nabla^2}{2m}-V^{\mathrm{ext}}(\mathbf{x})-2T^{2\mathrm{B}}(t)|\phi(\mathbf{x},t)|^2\right]\hat{\psi}'(\mathbf{x},t)=0, \tag{32}$$

with the Hermitian conjugate expression for the creation operator. We solve this equation by expanding the annihilation operator as

$$\hat{\psi}'(\mathbf{x},t)=\sum_{\mathbf{m}}{}'\phi_{\mathbf{m}}(\mathbf{x},t)\hat{\psi}'_{\mathbf{m}}, \tag{33}$$

where the Schrödinger operator $\hat{\psi}'_{\mathbf{m}}$ annihilates an atom in the harmonic-oscillator state with quantum number $\mathbf{m}$. We then expand also the functions $\phi_{\mathbf{m}}(\mathbf{x},t)$ in trap states by means of

$$\phi_{\mathbf{m}}(\mathbf{x},t)=\sum_{\mathbf{n}}{}'c^{\mathbf{m}}_{\mathbf{n}}(t)e^{-(i/\hbar)\epsilon_{\mathbf{n}}t}\chi_{\mathbf{n}}(\mathbf{x}), \tag{34}$$

and determine the equation of motion for the coefficients $c^{\mathbf{m}}_{\mathbf{n}}(t)$ from Eq. (32). This results in

$$\frac{dc^{\mathbf{m}}_{\mathbf{n}}(t)}{dt}=-\frac{2i}{\hbar}T^{2\mathrm{B}}(t)\sum_{\mathbf{n}}{}'V_{\mathbf{n},\mathbf{n}'}(t)c^{\mathbf{m}}_{\mathbf{n}'}(t)e^{-(i/\hbar)(\epsilon_{\mathbf{n}'}-\epsilon_{\mathbf{n}})t}, \tag{35}$$

with matrix elements given by

$$V_{\mathbf{n},\mathbf{n}'}(t)=\int d\mathbf{x}\chi^*_{\mathbf{n}}(\mathbf{x})|\phi(\mathbf{x},t)|^2\chi_{\mathbf{n}'}(\mathbf{x}), \tag{36}$$

which depend on time through the variational parameters in the Gaussian ansatz in Eq. (25) and the number of condensate atoms. These matrix elements can be calculated analytically and the result is given in Appendix. B. The advantage of the above approach is that we do not have to solve the equation for the derivative of $a_{\mathbf{n},\mathbf{n}'}(t,t')$ with respect to t' separately.

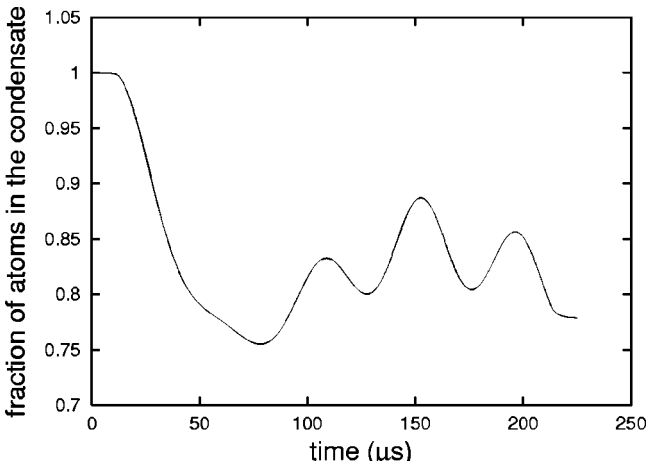

FIG. 6. The fraction of atoms in the condensate as a function of time for a calculation that includes only quantum evaporation. The initial number of condensate atoms is $N_{\mathrm{c}}(0)=16\,500$. The rise time $t_{\mathrm{rise}}=12.5\ \mu$s and the hold time is $t_{\mathrm{hold}}=200\ \mu$s. The scattering length is equal to $a=2000a_0$ during hold.

Putting the results together, we find for the coefficients in the expansion of the Green's function the expression

$$a_{\mathbf{n},\mathbf{n}'}(t,t')=\sum_{\mathbf{m}}{}'\ c^{\mathbf{m}}_{\mathbf{n}}(t)c^{\mathbf{m}}_{\mathbf{n}'}(t'). \tag{37}$$

With this Green's function we have performed simulations of the single-pulse experiments by Claussen *et al.* [33], of which the results are presented in the following section.

2. Results

We perform our calculations for the parameters of the experiment by Claussen *et al.* [33]. In particular, the frequencies of the external trapping potential are the same as in the preceding section. Figure 6 shows the fraction of atoms in the condensate as a function of time, for a pulse such that $t_{\mathrm{rise}}=12.5\ \mu$s and $t_{\mathrm{hold}}=200\ \mu$s. The magnetic field during the hold is $B=156.9$ G, which corresponds to a scattering length of $a=2000a_0$. The simulation shows that once the scattering length nearly takes on its largest value and the coupling between the condensate and the excited states is therefore largest, the condensate starts ejecting atoms. Part of these atoms then oscillate back and forth between the condensate and the excited states. The curve in Fig. 6 clearly contains several frequencies, since we are dealing with several excited states and thus a multimode Rabi oscillation. At the end of the pulse, the rate, i.e., the slope of the curve, becomes equal to zero because the coupling between the condensate and the excited states becomes equal to zero at the end of the pulse, where the scattering length is equal to zero.

To compare our results with the available experimental data, we calculate the number of atoms as a function of the

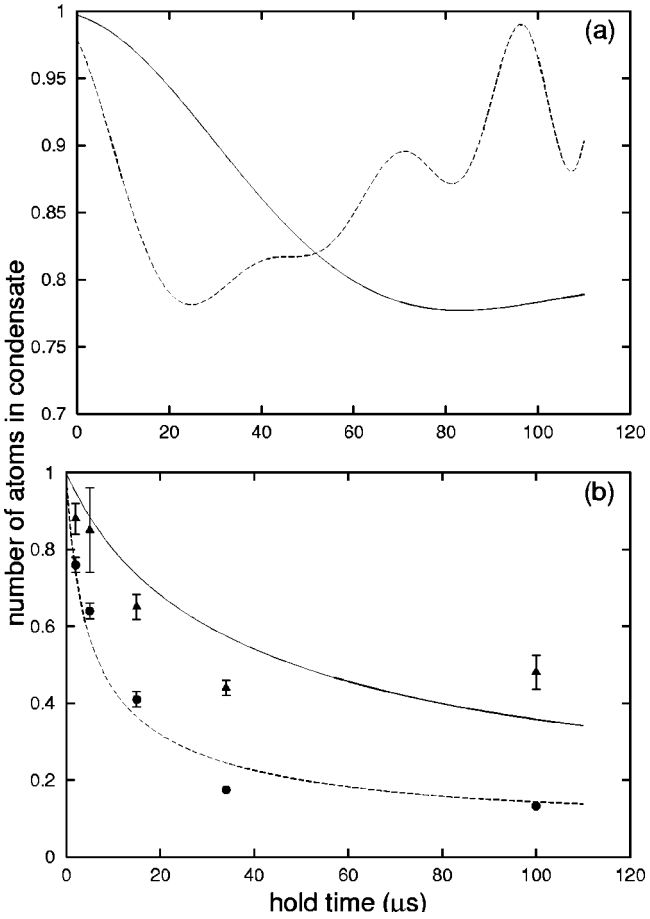

FIG. 7. Fraction of atoms in the condensate as a function of the hold time. The rise time is kept fixed at the value $t_{\mathrm{rise}}=12.5\ \mu$s. The initial number of condensate atoms is taken $N_c(0)=6100$ (solid line) and $N_c(0)=16\,500$ (dotted line). The scattering length is equal to $a=2000a_0$ during hold. (a) The result of the calculation that includes only quantum evaporation. (b) The calculation that includes both quantum evaporation and three-body recombination. The experimental points are taken from Ref. [33].

hold time t_{hold} and the rise time t_{rise}. Figure 7(a) shows the result of a calculation of the fraction of condensate atoms as a function of t_{hold}, with $t_{\mathrm{rise}}=12.5\ \mu$s fixed. The calculation is done for two different initial numbers of condensate atoms. The solid line displays the result for $N_c(0)=6100$ and the dashed line for $N_c(0)=16\,500$. Notice that the latter initially has a larger slope because the effective Rabi coupling between the condensate and the excited states is larger in this case. This is because of the fact that it is proportional to the condensate density.

The results of the simulation that includes only quantum evaporation, shown in Fig. 7(a), show an oscillation in the fraction of condensate atoms as a function of the hold time. This oscillation is not observed in experiment, because of the fact that three-body recombination plays an important role in this case since it becomes large near the resonance [47]. Therefore, we also want to perform a calculation that includes both quantum evaporation and three-body recombination. However, the magnetic-field dependence of the rate constant for this process is unknown. Nevertheless, we are

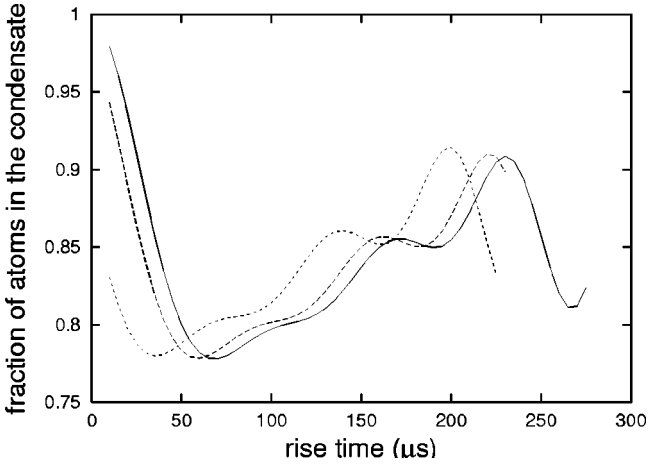

FIG. 8. Fraction of atoms in the condensate as a function of the rise time for a calculation that includes only quantum evaporation. The hold time is kept fixed at $t_{\mathrm{hold}}=1\ \mu$s (solid line), $t_{\mathrm{hold}}=5\ \mu$s (dashed line), and $t_{\mathrm{hold}}=15\ \mu$s (dotted line). The scattering length is equal to $a=2000a_0$ during hold.

able to make progress by realizing that the hold time is generally larger than the rise time for the experimental points shown in Fig. 7. Since experimentally three-body recombination is known to increase by orders of magnitude near the resonance [47], the contribution of three-body recombination will be most important during hold, where the magnetic field is closest to the resonance. This suggests that we only need to include it during hold. Note that for this approximation to be valid it is essential that the rise time is shorter that the hold time. If the rise time is larger than the hold time, the magnetic-field dependence of the three-body recombination rate constant is of importance, since the magnetic field is then time dependent for almost the entire pulse.

Figure 7(b) shows the result for a calculation that includes both quantum evaporation and three-body recombination, with a rate constant $K_3=3\times10^{-23}$ cm^6/s during hold. This value for the normal-component rate constant agrees with the order of magnitude of the experimental data [47]. This calculation shows good quantitative agreement with experiment for both initial numbers of condensate atoms.

Finally, we have calculated the number of atoms in the condensate as a function of the rise time. The result of this calculation is shown in Fig. 8, for various hold times. The solid line corresponds to $t_{\mathrm{hold}}=1\ \mu$s. The dashed and dotted lines correspond to hold times of 5 μs and 15 μs, respectively. The scattering length during hold is equal to $a=2000a_0$ for this simulation. For all the results in Fig. 8, the rise time of the pulse is larger than the hold time. This means that the magnetic-field dependence of the three-body recombination rate constant is very important in this case, since the magnetic field is varying most of the time. Fitting the dependence to the experiments is difficult due to the long times taken by the numerical computations. Therefore, we refrain from including three-body recombination in these simulations. Nevertheless, there is agreement with the experimental results regarding several aspects of our results. First, we find that the number of atoms increases with the rise time over some interval. This was also found in the experiment by

Claussen *et al.* [33]. Note that this fact cannot be explained by any loss process characterized by a rate constant because the amount of atom loss will then always be larger with longer times. Second, the minima of the curves in Fig. 8 shift to lower values of $t_{\rm rise}$ with longer hold times. This was also observed in the experiment by Claussen *et al.* [33]. These minima also occur on approximately the experimental values of $t_{\rm rise}$. The fact that in the experiment the minima become lower with increasing hold time can be explained by three-body recombination.

In conclusion, we have applied the generalized Gross-Pitaevskii equation to the recent single-pulse experiments by Claussen *et al.* [33]. We have shown that the number of atoms increases with time over some ranges. This cannot be understood in terms of conventional loss processes such as three-body recombination or dipolar decay. However, to obtain agreement with the available experimental data we had to include three-body recombination in our simulations. Due to the fact that the magnetic-field dependence of this process is completely unknown, we are not able to make a fit to experiment in all situations.

C. Atom-molecule coherence

Recent experimental and theoretical work has shown that atom-molecule coherence is of importance in the case of a double pulse in the magnetic field [29–32] . Therefore, we may expect it to have an important effect in the case of the single-pulse experiments as well. To make the discussion of these experiments more complete, we investigate the role of the molecules by means of a quantum field theory that we derived recently [28]. This theory incorporates the correct molecular binding energy and scattering properties of the atoms at the quantum level by using coupling constants that are dressed by ladder diagrams and by including the molecular self-energy. Introducing Heisenberg operators $\hat{\psi}_{\rm a}$ and $\hat{\psi}_{\rm m}$ that annihilate an atom and a bare molecule, respectively, the Hamiltonian for the atom-molecule system reads

$$i\hbar\frac{\partial\hat{\psi}_{\rm m}(\mathbf{x},t)}{\partial t}=\left[-\frac{\hbar^2\boldsymbol{\nabla}^2}{4m}+\delta(B(t))-g^2\frac{m^{3/2}}{2\pi\hbar^3}\times i\sqrt{i\hbar\frac{\partial}{\partial t}+\frac{\hbar^2\boldsymbol{\nabla}^2}{4m}}\right]\hat{\psi}_{\rm m}(\mathbf{x},t)+g\hat{\psi}_{\rm a}^2(\mathbf{x},t),$$

$$i\hbar\frac{\partial\hat{\psi}_{\rm a}(\mathbf{x},t)}{\partial t}=\left[-\frac{\hbar^2\boldsymbol{\nabla}^2}{2m}+T_{\rm bg}^{\rm 2B}\hat{\psi}_{\rm a}^{\dagger}(\mathbf{x},t)\hat{\psi}_{\rm a}(\mathbf{x},t)\right]\hat{\psi}_{\rm a}(\mathbf{x},t)+2g\hat{\psi}_{\rm a}^{\dagger}(\mathbf{x},t)\hat{\psi}_{\rm m}(\mathbf{x},t). \quad (38)$$

Here, $g=\hbar\sqrt{2\pi a_{\rm bg}\Delta B\Delta\mu/m}$ is the atom-molecule coupling constant and $\delta(B)=\Delta\mu(B(t)-B_0)$ denotes the detuning, i.e., the energy difference between two atoms and the bare molecule. It is determined by the difference in magnetic moment between the atoms and the bare molecule, which in the case of ^{85}Rb is equal to $\Delta\mu\approx-2.2\mu_{\rm B}$ [30].

At first glance, the term proportional to $\sqrt{i\hbar\partial/\partial t+\hbar^2\nabla^2/(4m)}$ may appear unexpected. It corresponds to the imaginary part of the self-energy of the bare molecule which arises physically from the fact that the molecular state interacts with the two-atom continuum. This affects both the wave function of the dressed molecule and its binding energy. By determining the pole of the molecular propagator for negative detuning, the latter can be shown to be given by [28]

$$\epsilon_{\rm m}(B)=\delta(B)+\frac{g^4m^3}{8\pi^2\hbar^6}\left[\sqrt{1-\frac{16\pi^2\hbar^6}{g^4m^3}\delta(B)}-1\right], \quad (39)$$

which reduces to $\epsilon_{\rm m}(B)=-\hbar^2/(m[a(B)]^2)$ for values of the magnetic field close to the resonance. Due to the coupling with the continuum of atoms, i.e., the open channel of the Feshbach problem, the molecular state is strongly affected and is given by

$$|\chi_{\rm m};\text{dressed}\rangle=\sqrt{Z(B)}|\chi_{\rm m};\text{bare}\rangle+\int\frac{d\mathbf{k}}{(2\pi)^3}C(\mathbf{k})|\mathbf{k},-\mathbf{k};\text{open}\rangle, \quad (40)$$

where the coefficients $C(\mathbf{k})$ are normalized as $\int d\mathbf{k}|C(\mathbf{k})|^2/(2\pi)^3=1-Z(B)$. It contains with an amplitude $\sqrt{Z(B)}$ the bare molecular state $|\chi_{\rm m};\text{bare}\rangle$. Moreover, because of the coupling to the two-atom continuum, the molecule acquires a nonzero component in the open channel [46]. The wave-function renormalization factor $Z(B)$ is given by [28]

$$Z(B)=\frac{1}{1+g^2m^{3/2}/(4\pi\hbar^3\sqrt{|\epsilon_{\rm m}(B)|})}, \quad (41)$$

which approaches 1 for values of the magnetic field far off-resonance, where the dressed molecular state reduces to the bare molecular state, as expected. However, for values of the magnetic field close to the resonance, it is much smaller than 1. In particular, for the case of the single-pulse experiments we always have that $Z(B)\ll1$, which implies that the magnetic moment of the dressed molecule is in very good approximation equal to twice the magnetic moment of an atom. For magnetically trapped atoms, this implies that the dressed molecule is subject to twice the trapping potential for the atoms. With respect to this remark, it is important to note that the result of the calculations of Kokkelmans and Holland [30] for the density of the molecular condensate should be multiplied by a factor $1/Z(B)\gg1$ to obtain the density of real dressed molecules, since these authors calculate the expectation value of the bare molecular-field operator $\langle\hat{\psi}_{\rm m}(\mathbf{x},t)\rangle$.

To bring out the physics of Eq. (38) more clearly, we introduce the operator $\hat{\psi}'_{\rm m}=\hat{\psi}_{\rm m}/\sqrt{Z(B)}$ that creates a dressed molecule, i.e., a molecule with an internal state as in Eq. (40). Since we intend to consider the situation where initially

all atoms are in the atomic condensate, we are allowed to make a mean-field approximation for the atomic field operator and consider only its expectation value. There are, however, no molecules present at the initial time and this requires a quantum treatment of the molecular field operators. The resulting equations for the atomic condensate wave function coupled to the dressed molecular-field read for the experimental conditions of interest

$$i\hbar\frac{\partial\phi_{\rm a}(\mathbf{x},t)}{\partial t}=\left[-\frac{\hbar^2\boldsymbol{\nabla}^2}{2m}+V^{\rm ext}(\mathbf{x})+T_{\rm bg}^{\rm 2B}|\phi_{\rm a}(\mathbf{x},t)|^2\right]\phi_{\rm a}(\mathbf{x},t)+2g\sqrt{Z(t)}\phi_{\rm a}^*(\mathbf{x},t)\hat{\psi}'_{\rm m}(\mathbf{x},t),$$

$$i\hbar\frac{\partial\hat{\psi}'_{\rm m}(\mathbf{x},t)}{\partial t}=\left[-\frac{\hbar^2\boldsymbol{\nabla}^2}{4m}+2V^{\rm ext}(\mathbf{x})+\epsilon_{\rm m}(t)\right]\hat{\psi}'_{\rm m}(\mathbf{x},t)+g\sqrt{Z(t)}\phi_{\rm a}^2(\mathbf{x},t), \tag{42}$$

where $\phi_{\rm a}\equiv\langle\hat{\psi}_{\rm a}\rangle$, $Z(t)\equiv Z(B(t))$, and $\epsilon_{\rm m}(t)\equiv\epsilon_{\rm m}(B(t))$. In the derivation of the above coupled equations, we have assumed that we are allowed to make an adiabatic approximation for the renormalization factor $Z(B)$ and that we can evaluate it at every time at the magnetic field $B(t)$. In principle, there are retardation effects due to the fact that the dressed molecular state does not change instantaneously. It turns out that these effects can be neglected if

$$\hbar\left|\frac{\partial\ln Z(t)}{\partial t}\right|\ll|\epsilon_{\rm m}(t)|, \tag{43}$$

which is fulfilled for almost the entire duration of most of the pulses in the experiments of Claussen *et al.* [33]. We come back to this point in the discussion at the end of the paper. In principle, the coupling between the two-atom continuum and the molecule also contains an incoherent part corresponding to the rogue-dissociation process considered by Mackie *et al.* [31]. The rate for this process will be small, however, under the condition given in Eq. (43). Moreover, the mean-field effects of the condensate on the thermal atoms will suppress this process even further. It can, in principle, be included straightforwardly and will take the form of a dissipation term in the equation for the molecular operator.

We solve the equations for the atomic condensate wave function coupled to the dressed molecular field by using for the condensate wave function again the Gaussian ansatz in Eq. (25), and by expanding the dressed molecular annihilation operator in harmonic-oscillator eigenstates, similar to the expansion in Eq. (33). As an initial condition, we assume that at $t=0$ only condensed atoms are present. The results of our calculations are shown in Figs. 9 and 10.

The calculations presented in Fig. 9 are performed for the same experimental conditions as in Fig. 7. This result clearly shows that a large fraction of atoms is coherently converted into molecules as a result of the fast ramp in the magnetic field and that these oscillate back and forth between the atomic condensate and the molecular states. Due to the fact

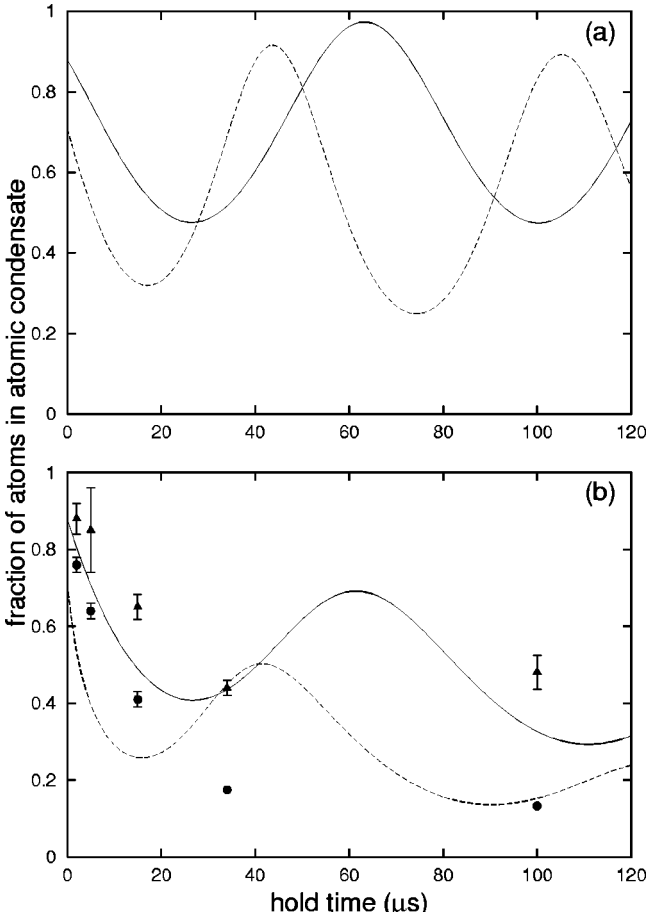

FIG. 9. Fraction of atoms converted in the condensate as a function of the hold time. The rise time is kept fixed at the value $t_{\rm rise}=12.5$ μs. The initial number of condensate atoms is taken $N_{\rm c}(0)=6100$ (solid line) and $N_{\rm c}(0)=16\,500$ (dashed line). The scattering length is equal to $a=2000a_0$ during hold. (a) The result of the calculation that includes only the coupling of the atomic condensate to the molecular field. (b) The calculation that includes both atom-molecule coupling and three-body recombination. The experimental points are taken from Ref. [33].

that the conversion of the atoms to the molecular states is coherent, the operator $\hat{\psi}'_{\rm m}(\mathbf{x},t)$ acquires a nonzero expectation value [48]. Figure 9(b) shows the results of simulations where also a three-body decay is taken into account in the same manner as in the preceding section. The normal-component rate constant is taken equal to $K_3=3\times10^{-23}$ cm^6/s. Interestingly, the initial decay without three-body recombination is already larger than the experimental data and by adding three-body recombination it is, therefore, impossible to make a fit to the experimental data. This is possibly the result of neglecting the retardation effects of the renormalization factor $Z(t)$ and the rogue-dissociation process, since the condition in Eq. (43) is violated for a significant fraction of the total duration of the pulse in this case. For the simulations presented in Fig. 10, this condition is violated only for a very small fraction of the total duration of the pulse for rise times larger that $t_{\rm rise}\approx50$ μs and is not violated at all for $t_{\rm rise}\geqslant150$ μs. Note that the effect of retardation and rogue dissociation lead to decoherence, which

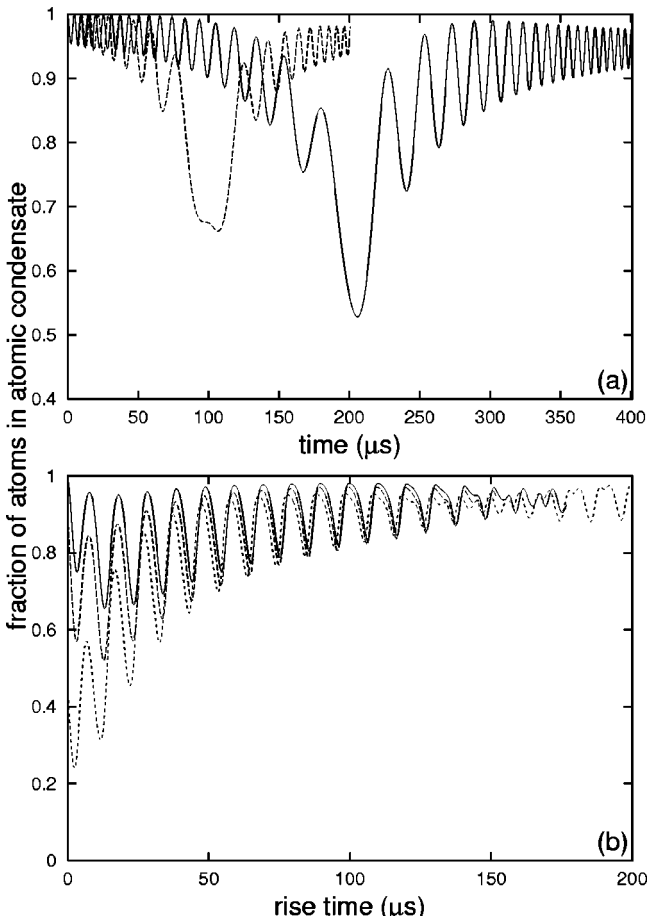

FIG. 10. Fraction of atoms in the atomic condensate for the situation where the atomic condensate is coupled to the molecular field. Initially, there are $N_c(0)=16\,500$ atoms and no molecules. The magnetic field is such that $a=2000a_0$ during the hold. (a) Fraction of atoms as a function of the real time for $t_{\rm rise}=200\ \mu$s (solid line) and $t_{\rm rise}=100\ \mu$s (dashed line). The hold time is equal to $t_{\rm hold}=1\ \mu$s for both pulses. (b) Fraction of atoms as a function of the rise time for different hold times of $t_{\rm hold}=1\ \mu$s (solid line), $t_{\rm hold}=5\ \mu$s (dashed line), and $t_{\rm hold}=15\ \mu$s (dotted line).

means that our calculations give an upper bound on the amount of molecules that are coherent with the atoms.

Figure 10(a) shows the result of two calculations for different rise time as a function of the total time. As expected, the number of atoms in the atomic condensate first oscillates with large frequency, since the dressed molecular binding energy is large here. As the magnetic field approaches values closer to the resonance, the frequency decreases. From Fig. 10(a) it is clear that only the smallest frequency, which also has the largest amplitude since the gas is then closest to resonance, gives a significant contribution to the frequency observed in the number of condensate atoms as a function of the rise time, because the larger frequencies with smaller amplitude average out. However, these oscillations are not observed in the experimental data of Ref. [33]. Introducing three-body recombination to fit the theory to experiment is impossible with pulses having relatively long rise times, for the same reasons as in the preceding section. Nevertheless, the amplitude of the oscillations is in this case, except for the longest hold time, comparable to that of the simulations where only quantum evaporation is included. This implies that for a thorough treatment of the single-pulse experiments, both atom-molecule coherence and quantum evaporation should be included. This is beyond the scope of the present paper but work in this direction is in progress.

IV. CONCLUSIONS

We have put forward a generalized Gross-Pitaesvkii equation that includes nonlocal terms which describe the quantum evaporation of the Bose-Einstein condensate. We have applied this equation to two experimental situations which make use of a Feshbach resonance to alter the interaction properties of the atoms. First, we have considered the case where the condensate undergoes a type-II collapse whose dynamics is mainly determined by the external trapping potential and have found good quantitative agreement with experiment. Second, we have considered the recent single-pulse experiments [33]. In general, we have also found agreement with experiment in this case, keeping in mind that the magnetic-field dependence of the three-body recombination rate constant is completely unknown. The latter is the first serious complication in the theoretical analysis. Apart from considering quantum evaporation we have also considered the role of atom-molecule coherence in the single-pulse experiments, by means of an adiabatic approximation to our effective quantum field theory for the description of Feshbach resonances [28]. In first instance, atom-molecule coherence appears to be an important effect. However, the second theoretical complication is that the adiabatic approximation, in general, overestimates the effect and does not take into account rogue dissociation [31]. Including this process damps out the Rabi oscillations between the atoms and molecules and leads to the production of energetic atoms that may contribute to the experimentally observed bursts [29]. Due to these two complications, a completely satisfying quantitative description of these experiments is still lacking. It should be mentioned that our calculations take into account the inhomogeneity of the trapped gas exactly and not in local-density approximation. In addition, we do not make a single-mode approximation either for the atomic condensate or the dressed molecules. In future work, we intend to consider quantum evaporation, rogue dissociation, and three-body recombination simultaneously to obtain more insight into these intriguing JILA experiments.

ACKNOWLEDGMENTS

It is a pleasure to thank Neil Claussen, Eric Cornell, Simon Cornish, Elisabeth Donley, and Carl Wieman for helpful remarks that have contributed to this paper.

APPENDIX A: RATE EQUATION FOR TYPE-II COLLAPSE

With the Gaussian ansatz for the condensate wave function and the semiclassical propagator for the ejected atoms, the final rate equation for the change in the number of atoms is given by

$$\frac{dN_c(t)}{dt} = -64i\sqrt{6}\hbar^3 a(t) N_c^{3/2}(t) \int_{-\infty}^{t} dt' \left\{ a(t') N_c^{3/2}(t') e^{-i[\theta_0(t)-\theta_0(t')]-(2i/\hbar)|\phi(\mathbf{0},(t+t')/2)|^2(t'-t)} \left[(m\pi q_r(t) q_r(t') \{ i q_r(t) q_r(t') \right.\right.$$

$$\times [(t-t')\dot{q}_r(t) - q_r(t)]\dot{q}_r(t') - q_r(t')\dot{q}_r(t)\} m^2 + 3m\hbar\{q_r^2(t) + (t'-t)[\dot{q}_r(t) q_r(t) - q_r(t')\dot{q}_r(t')] + q_r^2(t')\}$$

$$+ 9i\hbar^2(t'-t)) \sqrt{\frac{i q_z(t)\dot{q}_z(t')}{\omega_z} + 3} \sqrt{q_z(t) q_z(t') \left(3 - \frac{i m q_z(t')\dot{q}_z(t')}{\hbar} \right)}$$

$$\left.\left. \times \sqrt{\frac{m\dot{q}_z(t) q_z^3(t)}{3i\hbar m q_z(t)\dot{q}_z(t)} + q_z^2(t) + 3i\hbar \left(\frac{q_z^2(t')}{3i\hbar + m q_z(t')\dot{q}_z(t')} + \frac{t-t'}{m} \right)} \right]^{-1} \right\} - K_3 \frac{N_c^3(t)}{3\sqrt{3}\pi^3 q_r^4(t) q_z^2(t)}. \tag{A1}$$

Here, $q_r(t)$ and $q_z(t)$ denote the radial and axial widths of the condensate, respectively.

APPENDIX B: MATRIX ELEMENTS

In this appendix, we calculate the matrix elements $V_{\mathbf{n},\mathbf{n}'}(t)$ in Eq. (36). Because of the fact that we are dealing with a trapping potential that is symmetric around the z axis, the excited states factorize into a radial and an axial part. It is convenient to characterize the radial part of the excited states by the quantum numbers (n_r, m), where n_r counts the number of radial nodes in the wave function and m is the quantum number corresponding to the projection of the angular momentum on the z axis. The third quantum number n_z counts the number of nodes in the axial direction. In cylindrical coordinates, these states are given by [49]

$$\chi_{n_r,m,n_z}(r,\theta,z) \propto e^{-r^2/(2l_r^2)} |r|^m \times {}_1F_1(-n_r, |m|+1, (r/l_r)^2) e^{im\theta} H_{n_z}(z/l_z) e^{-z^2/(2l_z^2)}, \tag{B1}$$

where $l_i \equiv \sqrt{\hbar/(m\omega_i)}$. The Hermite polynomials are denoted by $H_n(x)$ and the confluent hypergeometric function is denoted by ${}_1F_1(p,q,x)$. The overlap integral with two functions of the form as in Eq. (B1) with a Gaussian of arbitrary width is, to the best of our knowledge, not tabulated. Nevertheless, we can make analytical progress by realizing that we only have to take into account the states with $m=0$, since the interaction conserves parity. The radial part of these states is given by

$$|\chi_{n_r}\rangle = \frac{1}{n_r!} \left(\frac{\hat{a}_x^\dagger - i\hat{a}_y^\dagger}{\sqrt{2}} \right)^{n_r} \left(\frac{\hat{a}_x^\dagger + i\hat{a}_y^\dagger}{\sqrt{2}} \right)^{n_r} |0\rangle, \tag{B2}$$

where the operator $(\hat{a}_x^\dagger - i\hat{a}_y^\dagger)/\sqrt{2}$ lowers the magnetic quantum number m of the angular momentum by 1. The operator $(\hat{a}_x^\dagger + i\hat{a}_y^\dagger)/\sqrt{2}$ raises this quantum number by 1. Here, the operators $\hat{a}_i^\dagger \equiv \sqrt{m\omega_i/(2\hbar)}[\hat{x}_i - i\hat{p}/(m\omega_i)]$ are the usual harmonic-oscillator creation operators. The ground state is denoted by $|0\rangle$. The creation operators commute and hence we can rewrite the radial wave function of the state as

$$|\chi_{n_r}\rangle = \sum_{n=0}^{n_r} \frac{\sqrt{(2n)!}\sqrt{(2(n_r-n))!}}{n!(n_r-n)!2^{n_r}} |2n\rangle_x |2m\rangle_y, \tag{B3}$$

where $|n\rangle_i$ denote the normalized eigenstates of the Hamiltonian $H_i = \hat{p}_i^2/(2m) + m\omega_i \hat{x}_i^2/2$ of the one-dimensional harmonic oscillator. In the derivation of this expression, we used Newton's binomium to rewrite the n_rth powers of the operators on the right-hand side of Eq. (B2) as a sum of n_r terms. With this result, the normalized wave functions of the excited states of interest are given by

$$\chi_{n_r,n_z}(\mathbf{x}) = \frac{1}{4^{n_r} n_z! 2^{n_z} \pi} \left[\sum_{n=0}^{n_r} \frac{1}{n!(n_r-n)!} e^{-(x^2+y^2)/(2l_r^2)} H_{2n}(x/l_r) H_{2(n_r-n)}(y/l_r) \right] e^{-z^2/(2l_z^2)} H_{n_z}(z/l_z). \tag{B4}$$

The overlap integrals of the two excited states of this form with a Gaussian of arbitrary width are tabulated [50]. The final result for the matrix elements is given by

$$V_{n_r,n_z;m_r,m_z}(t)=\frac{N_c(t)}{\pi^{3/2}l_r^2q_z(t)((q_r(t)/l_r)^2+1)}\sqrt{\frac{q_z^2(t)}{q_z^2(t)+l_z^2}}\frac{1}{2^{n_r+m_r}}\Bigg[\sum_{n=0}^{n_r}\sum_{m=0}^{m_r}\sum_{k=0}^{\min(2n,2m)}\sum_{l=0}^{\min[2(n_r-n),2(m_r-m)]}\frac{1}{n!(n_r-n)!}$$
$$\times\frac{1}{m!(m_r-m)!}\frac{(2n)!}{(2n-k)!}\frac{2(n_r-n)}{[2(n_r-n)-l]!}\binom{2m}{k}\binom{2(m_r-m)}{l}$$
$$\times[2(m+n-k)-1]!![2(n_r+m_r-n-m-l)-1]!!\{[q_r(t)/l_r]^2+1\}^{k+l-n_r-m_r}\Bigg]$$
$$\times\Bigg[\sum_{q}^{\min(n_z,m_z)}\frac{\sqrt{n_z!m_z!}}{q!(n_z-q)!(m_z-q)!}\{[q_z(t)/l_z]^2+1\}^{q/2-(m_z+n_z)/4}(n_z+m_z-2q-1)!!\Bigg], \tag{B5}$$

if n_z+m_z is even, otherwise it is equal to zero.

[1] See, for instance, J.J. Sakurai, *Modern Quantum Mechanics* (Addison-Wesley, New York, 1994).
[2] H. Feshbach, Ann. Phys. (N.Y.) **19**, 287 (1962).
[3] W.C. Stwalley, Phys. Rev. Lett. **37**, 1628 (1976).
[4] E. Tiesinga, B.J. Verhaar, and H.T.C. Stoof, Phys. Rev. A **47**, 4114 (1993).
[5] S. Inouye, M.R. Andrews, J. Stenger, H.-J. Miesner, D.M. Stamper-Kurn, W. Ketterle, Nature (London) **392**, 151 (1998).
[6] Ph. Courteille, R.S. Freeland, D.J. Heinzen, F.A. van Abeelen, B.J. Verhaar, Phys. Rev. Lett. **81**, 69 (1998).
[7] J.L. Roberts, N.R. Claussen, J.P. Burke, Jr., C.H. Greene, E.A. Cornell, and C.E. Wieman, Phys. Rev. Lett. **81**, 5109 (1998).
[8] V. Vuletić, A.J. Kerman, C. Chin, and S. Chu, Phys. Rev. Lett. **82**, 1406 (1999).
[9] S.L. Cornish, N.R. Claussen, J.L. Roberts, E.A. Cornell, C.E. Wieman, Phys. Rev. Lett. **85**, 1795 (2000).
[10] P.A. Ruprecht, M.J. Holland, K. Burnett, and M. Edwards, Phys. Rev. A **51**, 4704 (1995).
[11] E.V. Shuryak, Phys. Rev. A **54**, 3151 (1996).
[12] H.T.C. Stoof, J. Stat. Phys. **87**, 1353 (1997).
[13] M. Houbiers and H.T.C. Stoof, Phys. Rev. A **54**, 5055 (1996).
[14] T. Bergeman, Phys. Rev. A **55**, 3658 (1997).
[15] C.C. Bradley, C.A. Sackett, J.J. Tollett, and R.G. Hulet, Phys. Rev. Lett. **75**, 1687 (1995); C.C. Bradley, C.A. Sackett, and R.G. Hulet, *ibid.* **78**, 985 (1997).
[16] C.A. Sackett, H.T.C. Stoof, and R.G. Hulet, Phys. Rev. Lett. **80**, 2031 (1998).
[17] C.A. Sackett, J.M. Gerton, M. Welling, and R.G. Hulet, Phys. Rev. Lett. **82**, 876 (1999).
[18] R.A. Duine and H.T.C. Stoof, Phys. Rev. A **65**, 013603 (2002).
[19] J.M. Gerton, D. Strekalov, I. Prodan, and R.G. Hulet, Nature (London) **408**, 692 (2000).
[20] J.L. Roberts, N.R. Claussen, S.L. Cornish, E.A. Donley, E.A. Cornell, and C.E. Wieman, Phys. Rev. Lett. **86**, 4211 (2001).
[21] E.A. Donley, N.R. Claussen, S.L. Cornish, J.L. Roberts, E.A. Cornell, and C.E. Wieman, Nature (London) **412**, 295 (2001).
[22] Yu. Kagan, A.E. Muryshev, and G.V. Shlyapnikov, Phys. Rev. Lett. **81**, 933 (1998).
[23] M. Ueda and K. Huang, Phys. Rev. A **60**, 3317 (1999).
[24] A. Eleftheriou and K. Huang, Phys. Rev. A **61**, 043601 (2000).
[25] S.K. Adhikari, Phys. Lett. A **296**, 145 (2002); Phys. Rev. A **66**, 013611 (2002).
[26] H. Saito and M. Ueda, Phys. Rev. A **65**, 033624 (2002).
[27] L. Santos and G.V. Shlyapnikov, Phys. Rev. A **66**, 011602(R) (2002).
[28] R.A. Duine and H.T.C. Stoof, J. Opt. B: Quantum Semiclassical Opt. **5**, S212 (2003).
[29] E.A. Donley, N.R. Claussen, S.T. Thompson, and C.E. Wieman, Nature (London) **417**, 529 (2002).
[30] S.J.J.M.F. Kokkelmans and M.J. Holland, Phys. Rev. Lett. **89**, 180401 (2002).
[31] M. Mackie, K.-A. Suominen, and J. Javanainen, Phys. Rev. Lett. **89**, 180403 (2002).
[32] T. Köhler, T. Gasenzer, and K. Burnett, Phys. Rev. A **67**, 013601 (2002).
[33] N.R. Claussen, E.A. Donley, S.T. Thompson, and C.E. Wieman, Phys. Rev. Lett. **89**, 010401 (2002).
[34] R.A. Duine and H.T.C. Stoof, Phys. Rev. Lett. **86**, 2204 (2001).
[35] J. Schwinger, J. Math. Phys. **2**, 407 (1961).
[36] L.V. Keldysh, Zh. Éksp. Teor. Fiz. **47**, 1515 (1964) [Sov. Phys. JETP **20**, 1018 (1965)].
[37] H.T.C. Stoof, Phys. Rev. Lett. **66**, 3148 (1991); Phys. Rev. A **45**, 8398 (1992).
[38] H.T.C. Stoof, Phys. Rev. Lett. **78**, 768 (1997).
[39] H.T.C. Stoof, J. Low Temp. Phys. **114**, 11 (1999).
[40] S.L. Cornish and C. E. Wieman (private communication).
[41] V.M. Perez-Garcia, H. Michinel, J.I. Cirac, M. Lewenstein, and P. Zoller, Phys. Rev. Lett. **77**, 5320 (1996).
[42] A.J. Moerdijk, H.M.J.M. Boesten, and B.J. Verhaar, Phys. Rev. A **53**, 916 (1996).
[43] P.O. Fedichev, M.W. Reynolds, and G.V. Shlyapnikov, Phys. Rev. Lett. **77**, 2921 (1996).
[44] B.D. Esry, C.H. Greene, and J.P. Burke, Jr., Phys. Rev. Lett. **83**, 1751 (1999).
[45] E. Braaten and H.-W. Hammer, Phys. Rev. Lett. **87**, 160407 (2001).
[46] P.D. Drummond, K.V. Kheruntsyan, and H. He, Phys. Rev. Lett. **81**, 3055 (1998); K.V. Kheruntsyan and P.D. Drummond, Phys. Rev. A **58**, R2676 (1998).

[47] J.L. Roberts, N.R. Claussen, S.L. Cornish, and C.E. Wieman, Phys. Rev. Lett. **85**, 728 (2000).

[48] E. Timmermans, P. Tommasini, H. Hussein, and A. Kerman, Phys. Rep. **315**, 199 (1999).

[49] See, for instance, B.H. Bransden and C.J. Joachain, *Introduction to Quantum Mechanics* (Longman Scientific & Technical, Harlow, New York, 1989), p. 353.

[50] I.S. Gradshteyn and I.M. Ryzik, *Table of Integrals, Series and Products* (Academic Press, New York, 1994).

[51] More precisely, such a supernova is called a type-Ia supernova. The proper classification scheme of supernovas is based on the characteristics of their spectra.

[52] In Ref. [34] we used the form $\phi(\mathbf{x},t) = (1/(2\pi))^3 \int d\mathbf{k} e^{-(i/\hbar)\epsilon(\mathbf{k})t} \phi(\mathbf{k},t)$, where $\phi(\mathbf{k},t)$ is the Fourier transform of the Gaussian ansatz, and assumed the energy of a condensate atoms to be negligibly small with respect to the energy of an ejected atom. Moreover, in the retarded propagator of the ejected atoms we neglected the mean-field energy with respect to the kinetic energy of the ejected atoms. Here we go beyond these approximations.